Optical Spectra and Electronic Band Structure Calculations of β''-$(ET)_2SF_5RSO_3$ (R = CH_2CF_2, $CHFCF_2$, and CHF): Changing Electronic Properties by Chemical Tuning of the Counterion

B. R. Jones, I. Olejniczak,* J. Dong, J. M. Pigos, Z. T. Zhu, A. D. Garlach, and J. L. Musfeldt

Department of Chemistry, State University of New York at Binghamton, Binghamton, New York 13902-6016

H.-J. Koo and M.-H. Whangbo

Department of Chemistry, North Carolina State University, Raleigh, North Carolina 27695

J. A. Schlueter, B. H. Ward, E. Morales, and A. M. Kini

Chemistry and Materials Science Divisions, Argonne National Laboratory, Argonne, Illinois 60439

R. W. Winter, J. Mohtasham, and G. L. Gard

Department of Chemistry, Portland State University, Portland, Oregon 97207

Received April 27, 2000. Revised Manuscript Received June 16, 2000

We report the polarized infrared reflectance spectra, optical conductivity, and electronic band structure of metallic β''-$(ET)_2SF_5CHFSO_3$ and compare our results with those of the β''-$(ET)_2SF_5CH_2CF_2SO_3$ superconductor and the β''-$(ET)_2SF_5CHFCF_2SO_3$ metal/insulator material. We discuss the electronic structure of these organic molecular solids in terms of band structure, many-body effects, and disorder. On the basis of spectral similarities between the superconductor and metallic salts and structural differences in the anion pocket of all three, we conclude that the unusual electronic excitations observed in the β''-$(ET)_2SF_5CHFCF_2SO_3$ metal/insulator material are not caused by electron correlation but are due to disorder-related localization.

I. Introduction

The discovery of superconductivity and other competing ground states in ET (bis(ethylenedithio)tetrathiafulvalene)-containing complexes has stimulated extensive experimental studies of these materials.[1−3] Attempts to tune the physical properties of these compounds have been fruitful. In particular, the incorporation of large, discrete, chemically tunable anions with the ET cation allows the exploration of the effect of slight anion modifications on the physical properties of the molecular solid.[4,5] The β''-$(ET)_2SF_5RSO_3$ (R = CH_2CF_2, $CHFCF_2$, and CHF) system is an example of this effort; superconducting, semiconducting, or metallic ground states have been observed depending on R.[6] It is the β''-$(ET)_2SF_5CHFSO_3$ metal and a comparison with the β''-$(ET)_2SF_5CH_2CF_2SO_3$ superconductor and the β''-$(ET)_2SF_5CHFCF_2SO_3$ metal/insulator material that are of interest here.

The β''-$(ET)_2SF_5RSO_3$ family consists of alternating layers of ET cations and $SF_5RSO_3^-$ anions. The ET molecules form stacks along the crystallographic *a* direction, with close, short intermolecular contacts along *b*. Figure 1 shows the structure of the anion pocket and the resistivity of the three materials studied. In β''-$(ET)_2SF_5CH_2CF_2SO_3$, the ethylene end groups of the ET cation form hydrogen bonds with the peripheral fluorines and oxygens of the anion. It is interesting that there is no intermolecular contact between the inner fluorines of the anion and the hydrogens of the donor molecules. The anion itself contains no chiral carbon, and the anion pocket of the superconductor is ordered.

* Permanent address: Institute of Molecular Physics, Polish Academy of Sciences, Smoluchowskiego 17, Poznan, Poland.

(1) Ishiguro, T.; Yamaji, K.; Saito, G. *Organic Superconductors*, 2nd ed.; Springer-Verlag: Berlin, 1997.

(2) Wosnitza, J. *Fermi Surfaces of Low Dimensional Organic Metals and Superconductors*; Springer-Verlag: Berlin, 1996.

(3) Williams, J. M.; Ferraro, J. R.; Carlson, K. D.; Geiser, U.; Wang, H. H.; Kini, A. M.; Whangbo, M. H. *Organic Superconductors*; Prentice Hall: Englewood Cliffs, NJ, 1992.

(4) Schlueter, J. A.; Carlson, K. D.; Geiser, U.; Wang, H. H.; Williams, J. M.; Kwok, W.-K.; Fendrich, J. A.; Welp, U.; Keane, P. M.; Dudek, J. D.; Komosa, A. S.; Naumann, D.; Roy, T.; Schirber, J. E.; Bayless, W. R.; Dodrill, B. *Physica C* **1994**, *233*, 379.

(5) Schlueter, J. A.; Williams, J. M.; Geiser, U.; Dudek, J. D.; Kelly, M. E.; Sirchio, S. A.; Carlson, K. D.; Naumann, D.; Roy, T.; Campana, C. F. *Adv. Mater.* **1995**, *7*, 634.

(6) Ward, B. H.; Schlueter, J. A.; Geiser, U.; Wang, H. H.; Morales, E.; Parakka, J.; Thomas, S. Y.; Williams, J. M.; Nixon, P. G.; Winter, R. W.; Gard, G. L.; Koo, H. J.; Whangbo, M. H. *Chem. Mater.* **2000**, *12*, 343.

10.1021/cm000349l CCC: $19.00
Published on Web 08/21/2000

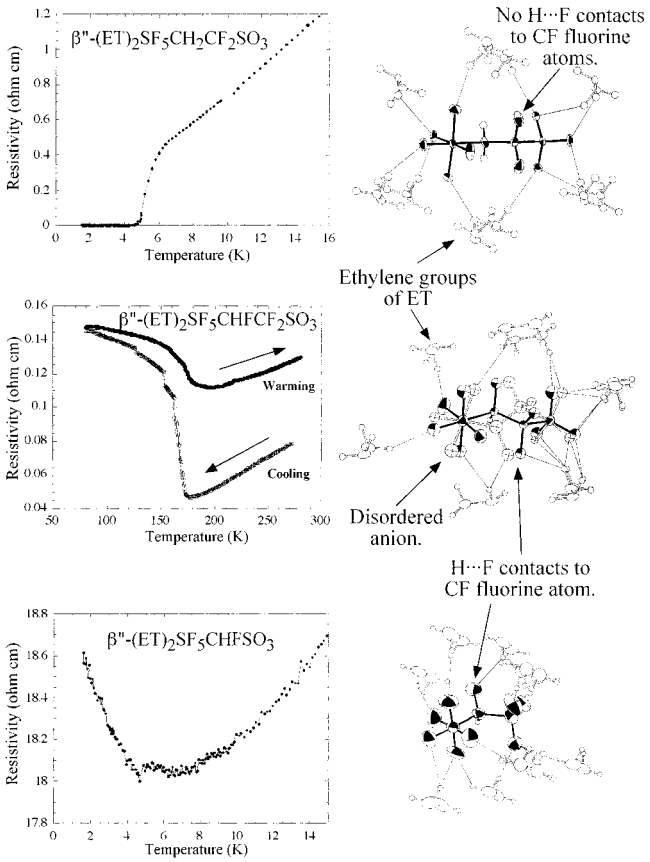

Figure 1. Structure of the anion pocket in β''-(ET)$_2$SF$_5$CH$_2$CF$_2$SO$_3$, β''-(ET)$_2$SF$_5$CHFCF$_2$SO$_3$, and β''-(ET)$_2$SF$_5$CHFSO$_3$ at 300 K. Also displayed is the temperature-dependent resistivity for each of the aforementioned compounds.]

In the resistivity versus temperature plot, the resistivity drops to zero at 5 K, indicating the T_c of this first fully organic superconductor.[7]

In the metal/insulator material, β''-(ET)$_2$SF$_5$CHFCF$_2$SO$_3$, the chiral carbon of the anion causes disorder in the anion pocket, as the peripheral oxygen and fluorine atoms compete with the interior fluorine atoms of the anion for the intermolecular contacts with the ethylene end groups of the ET donor molecules. Figure 1 illustrates the disordered arrangement of the SF$_5$CHFCF$_2$SO$_3^-$ anions and shows the two possible configurations that lock in at low temperature. The metal → insulator transition near 180 K and the strong hysteresis in the resistivity plot for the β''-(ET)$_2$SF$_5$CHFCF$_2$SO$_3$ salt are related to the disordered anion pocket.[8]

In general, the metallic β''-(ET)$_2$SF$_5$CHFSO$_3$ salt is quite similar in the cation layer structure to both the superconductor and metal/insulator materials but again differs in the structure of the anion pocket. Like SF$_5$CHFCF$_2$SO$_3^-$, the anion possesses a chiral carbon atom and there are some intermolecular contacts between the interior flourine and the ET donor molecule, yet the anion pocket of the metallic salt is fairly well-ordered, making it similar to the superconductor in this respect. This material remains metallic to low temperature where an upward turn in the resistivity is observed near 6 K, the cause of which is not well understood.[6]

Infrared and optical measurements of both the R = CH_2CF_2 superconductor and the R = $CHFCF_2$ metal/insulator materials have been reported previously.[9,10] The $\perp b$ optical response of the metal/insulator material reveals a shoulder at 4800 cm^{-1} and a strong electronic band around 9500 cm^{-1} that are not observed in the spectrum of the superconductor. These $\perp b$ excitations observed for β''-(ET)$_2$SF$_5$CHFCF$_2$SO$_3$ cannot be explained by extended Hückel tight binding band structure calculations, and localized models do not predict strong excitations in this direction either.[11−16] It has been suggested that these transverse excitations may be either correlation- or disorder-related.[10]

To gain further information on the nature of the electronic processes in this class of materials, we have investigated the polarized infrared and optical response of metallic β''-(ET)$_2$SF$_5$CHFSO$_3$. We compare the results of the metallic salt with those of the β''-(ET)$_2$SF$_5$CH$_2$CF$_2$SO$_3$ superconductor[9] and the β''-(ET)$_2$SF$_5$CHFCF$_2$SO$_3$ metal/insulator material and discuss the optical data from the viewpoint of electronic band structure calculations. Our overall goal is to understand the relationship between the chemical structure of the anion and the ground-state physical properties in the β''-(ET)$_2$SF$_5$RSO$_3$ family and to determine the nature of the near-infrared electronic excitations found in the metal/insulator (R = $CHFCF_2$) material.

II. Experimental Section

High-quality single crystals of β''-(ET)$_2$SF$_5$CH$_2$CF$_2$SO$_3$, β''-(ET)$_2$SF$_5$CHFCF$_2$SO$_3$, and β''-(ET)$_2$SF$_5$CHFSO$_3$ were grown via electrochemical techniques in an H-cell at Argonne National Laboratory.[6−8] Typical dimensions of the R = CHF material studied here were 1.0 × 1.8 × 0.3 mm^3. Of the three samples, R = CHF had the poorest crystal quality, while the R = CH_2CF_2 crystal was the best.

Polarized middle and near-infrared reflectance measurements on β''-(ET)$_2$SF$_5$CHFSO$_3$ were performed using a Bruker Equinox 55 FTIR spectrometer (650−15000 cm^{-1}) in combination with a Bruker IR Scope II infrared microscope and a 15× objective. Nitrogen-cooled detectors (MCT and InSb) as well as a Si diode detector and standard polarizers were used to cover the aforementioned energy range. Data were collected at 300 K. The experimental conditions for β''-(ET)$_2$SF$_5$CH$_2$CF$_2$SO$_3$ and β''-(ET)$_2$SF$_5$CHFCF$_2$SO$_3$ are given in refs 9 and 10, respectively.

The frequency range of the measurement allows us to make a Kramers−Kronig analysis of the power reflectance to obtain

(7) Geiser, U.; Schlueter, J. A.; Wang, H. H.; Kini, A. M.; Williams, J. M.; Sche, P. P.; Zakowicz, J. I.; VanZile, M. L.; Dudek, J. D. *J. Am. Chem. Soc.* **1996**, *118*, 9996.
(8) Schlueter, J. A.; Ward, B. H.; Geiser, U.; Wang, H. H.; Kini, A. M.; Parakka, J.; Morales, E.; Koo, H. J.; Whangbo, M. H.; Winter, R. W.; Mohtasham, J.; Gard, G. L. *J. Mater. Chem.*, manuscript in preparation.
(9) Dong, J.; Musfeldt, J. L.; Schlueter, J. A.; Williams, J. M.; Gard, G. L. *Synth. Met.* **1999**, *103*, 1892.
(10) Olejniczak, I.; Jones, B. R.; Zhu, Z.; Dong, J.; Musfeldt, J. L.; Schlueter, J. A.; Morales, E.; Geiser, U.; Nixon, P. G.; Winter, R. W.; Gard, G. L. *Chem. Mater.* **1999**, *11*, 3160.
(11) Tajima, H.; Yakushi, K.; Kuroda, H.; Saito, G. *Solid State Commun.* **1985**, *56*, 159.
(12) Ugawa, A.; Ojima, G.; Yakushi, K.; Kuroda, H. *Phys. Rev. B* **1988**, *38*, 5122.
(13) Yartsev, V. M.; Drozdova, O. O.; Semkin, V. N.; Vlasova, R. M. *J. Phys. I* **1996**, *6*, 1673.
(14) McKenzie, R. H. *Comments Condens. Mater. Phys.* **1998**, *18*, 309.
(15) Bulka, B. R. Proceedings of the 1998 Conference on Molecular Crystals, Gdansk, Poland. *Mol. Phys. Rep.* **1999**, *25*, 41−50.
(16) Fortunelli, A.; Painelli, A. *Phys. Rev. B* **1997**, *55*, 16088.

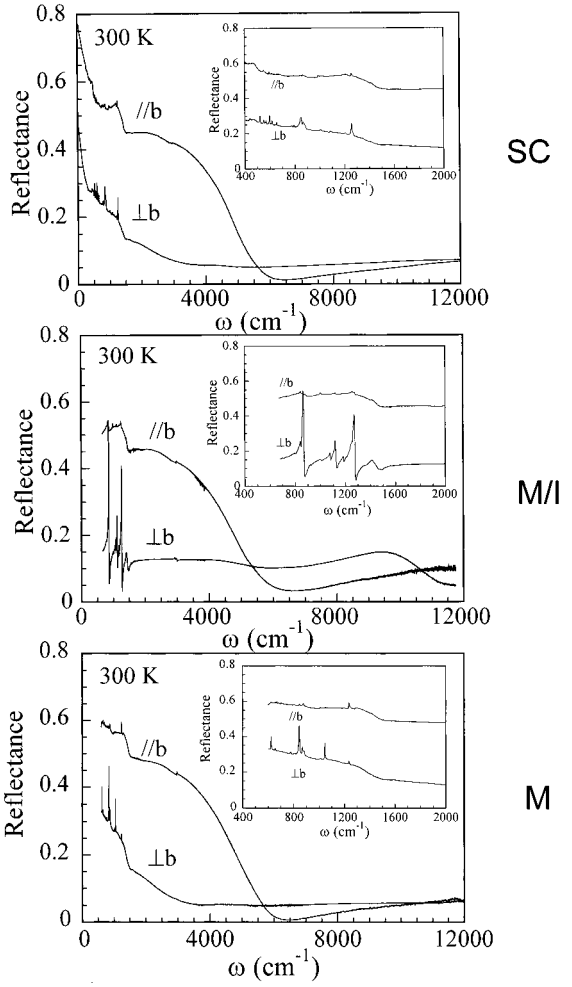

Figure 2. Polarized infrared reflectance of β''-$(ET)_2SF_5CH_2CF_2SO_3$, β''-$(ET)_2SF_5CHFCF_2SO_3$, and β''-$(ET)_2SF_5CHFSO_3$ at 300 K. Both ||*b* and ⊥*b* polarizations are shown. The insets display close-up views of the low-frequency vibrational structure in the reflectance response of each material.

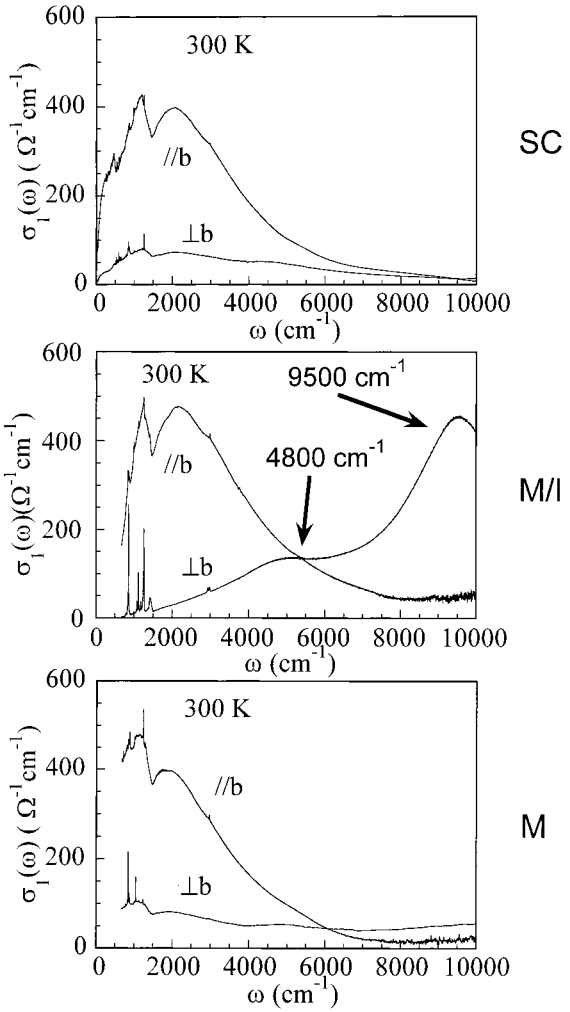

Figure 3. Room-temperature frequency-dependent conductivity of β''-$(ET)_2SF_5CH_2CF_2SO_3$, β''-$(ET)_2SF_5CHFCF_2SO_3$, and β''-$(ET)_2SF_5CHFSO_3$ at 300 K. Arrows highlight the 4800 and 9500 cm^{-1} electronic excitations.-

the optical constants of the material. These include the frequency dependent conductivity, $\sigma_1(\omega)$, the dielectric constant, $\epsilon_1(\omega)$, and the effective mass, $m^*(\omega)$.[17] The exponent for the high-frequency extrapolation to the Kramers−Kronig phase shift integral was carefully chosen to mimic the data for the superconductor when it is cut at 12 000 cm^{-1} and compared with that obtained using the full spectrum. This method necessitated a recalculation of the optical constants of the metal/insulator material, which changed some details, but the essential features remained the same.[10] The low-frequency extrapolation was made as a constant, which is appropriate for a semiconducting sample.[17]

III. Results

A. Spectral Results. Figure 2 displays the 300 K reflectance of β''-$(ET)_2SF_5RSO_3$ in the two principle polarization directions for all three samples of interest. In general, the ||*b* reflectance is significantly larger than that in the ⊥*b* direction (~||*a*, i.e., ET stack direction) at low energy. There is a strong similarity in the overall shape of the ||*b* spectra of all three materials; only small differences in the reflectance levels are observed.[18]

In the ⊥*b* polarization, the reflectance spectra of the superconductor (R = CH_2CF_2) and the metallic (R = CHF) sample are very similar. Both display overdamped behavior (though the level is slightly higher for the metal at low frequency, analogous to that found in the ||*b* polarization) and a barely discernible slope change near 4800 cm^{-1}. The reflectance spectrum of the metal/insulator material in the ⊥*b* direction is much different from those of the other two samples. The overall level is low and flat in the middle infrared, characteristic of a one-dimensional semiconductor. The weak excitation at 4800 cm^{-1} found in both the superconductor and metal is observed more strongly here, and there is a noticeable electronic feature above 9000 cm^{-1}. Although the vibrational features are stronger in the ⊥*b* than the ||*b* polarization for all three materials, these modes are the most pronounced in the metal/insulator (R = $CHFCF_2$) compound.

The 300 K frequency dependent conductivities of β''-$(ET)_2SF_5CH_2CF_2SO_3$, β''-$(ET)_2SF_5CHFCF_2SO_3$, and β''-$(ET)_2SF_5CHFSO_3$ are shown in Figure 3. All three samples show a strong electronic excitation in the ||*b*

(17) Wooten, F. *Optical Properties of Solids*; Academic Press: New York, 1972.

(18) Compared to that of the superconductor, the ||*b* reflectance level of the metal/insulator material matches almost exactly in the middle-infrared yet is slightly higher in the near-infrared. In contrast, the reflectance level of the metallic sample tracks that of the superconductor quite well in the near-infrared yet is noticeably higher in the middle-infrared.

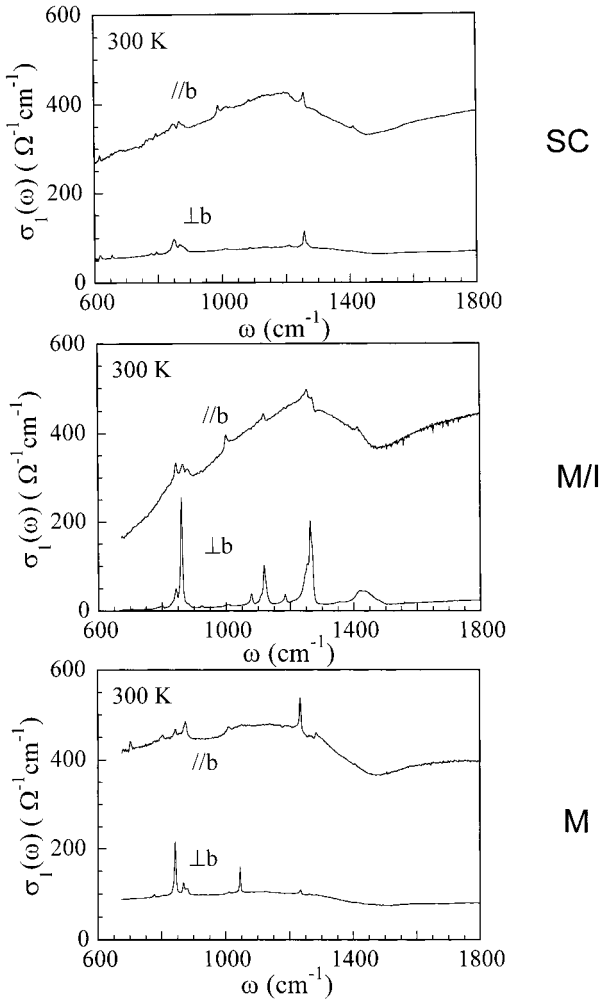

Figure 4. Close-up views of the vibrational structure from the optical conductivity spectra of β″-(ET)$_2$SF$_5$CH$_2$CF$_2$SO$_3$, β″-(ET)$_2$SF$_5$CHFCF$_2$SO$_3$, and β″-(ET)$_2$SF$_5$CHFSO$_3$ at 300 K.-

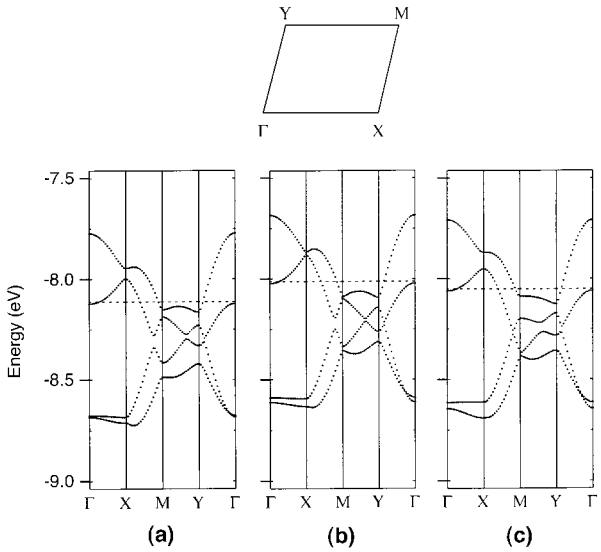

Figure 5. Extended Hückel tight binding (EHTB) band structure calculations for (a) β″-(ET)$_2$SF$_5$CH$_2$CF$_2$SO$_3$, (b) β″-(ET)$_2$SF$_5$CHFCF$_2$SO$_3$, and (c) β″-(ET)$_2$SF$_5$CHFSO$_3$. The Fermi level of the metallic state of each material is indicated by a dashed line.

direction centered at ≈2200 cm^{-1}. The conductivity then drops gradually, and there are no other major features in any of the three spectra in the frequency range of interest here. The ||*b* effective masses were calculated from a partial sum rule on the optical conductivity and found to be $m^*_b \approx 1.6m_e$, $m^*_b \approx 1.4m_e$, and $m^*_b \approx 1.7m_e$ for the superconductor, metal/insulator, and metal, respectively.

Optically, the metal/insulator material (R = CHFCF$_2$) is highly anisotropic and the ⊥*b* response differs dramatically from those of the other two compounds. The metal/insulator sample shows a shoulder around 4800 cm^{-1} and a broad, strong electronic excitation in this direction centered at 9500 cm^{-1}. Both the superconductor and the metal display a hint of the same electronic feature at 4800 cm^{-1} but show no evidence of the excitation at 9500 cm^{-1}. We will focus our attention on these two excitations. Close-up views of the vibrational structure in the optical conductivity spectra are shown in Figure 4.

B. Calculated Band Structure. The electronic band structures of β″-(ET)$_2$SF$_5$CH$_2$CF$_2$SO$_3$, β″-(ET)$_2$SF$_5$CHFCF$_2$SO$_3$, and β″-(ET)$_2$SF$_5$CHFSO$_3$ calculated by using the extended Hückel tight binding method are presented in Figure 5, where only the bands resulting primarily from the highest occupied molecular orbital of each ET are shown. The Fermi levels of the metallic states of these compounds are indicated by the dashed lines. In general, the electronic structures of these three salts are quite similar. This is not surprising because the crystallographic parameters of the three materials are nearly identical, and so are the arrangements of the ET donor molecules in their cation layers. Consequently, the higher energy ⊥*b* excitations observed for β″-(ET)$_2$SF$_5$CHFCF$_2$SO$_3$ cannot be explained by electronic band structure calculations and hence should be associated with a phenomenon that breaks the translational symmetry.

IV. Discussion

A. Electronic Spectra. Overall, the weakly conducting response in the ||*b* direction is very similar in all three β″-(ET)$_2$SF$_5$RSO$_3$ materials and characteristic of other known β-type conductors.[19,20] In terms of an electronic band structure model, the excitation at ≈2200 cm^{-1} found in the optical conductivity of all three salts can be interpreted as an interband transition.[21] Such a low-energy localization may also be accounted for within a Hubbard or other localized model.[9,10]

Both the transverse optical conductivity (Figure 3) and a ⊥*b* partial sum rule calculation (not shown) indicate that the metal and superconductor have moderate low-frequency oscillator strength, indicative of weakly bound or nearly metallic carriers. In contrast, the metal/insulator material displays very little intensity in N_{eff} (m/m^*)[22] at low energy, and the majority of its oscillator strength lies in the near-infrared regime,

(19) Jacobsen, C. S.; Williams, J. M.; Wang, H. H. *Solid State Commun.* **1985**, *54*, 937.
(20) Jacobsen, C. S.; Tanner, T. B.; Williams, J. M.; Geiser, U.; Wang, H. H. *Phys. Rev. B* **1987**, *35*, 9605.
(21) Koo, H.-J.; Whangbo, M.-H.; Dong, J.; Olejniczak, I.; Musfeldt, J. L.; Schlueter, J. A.; Geiser, U. *Solid State Commun.* **1999**, *112*, 403.
(22) Note that the partial sum rule gives the area under $\sigma_1(\omega)$. N_{eff} is the number of carriers participating in the optical transition, m^* is the effective mass, and m is the mass of an electron.

Table 1. Vibrational Assignments in the 300 K Spectra of β''-$(ET)_2SF_5RSO_3$[a,b]

ω (cm^{-1}) $\perp b$			assignment		
SC	M/I	M	SC	M/I	M
852	845	840	anion, SF_5 stretching	anion, SF_5 stretching	anion, SF_5 stretching
875	865	860	ET related ν_{60} (B_{3g})	ET related ν_{60} (B_{3g})	ET related ν_{60} (B_{3g})
1093	1090, 1120	1048	anion, SF_3 stretching	anion, SO_3 stretch + ET ν_{21} (B_{1g})	anion, SF_3 stretching
1190			ET related ν_{38} (B_{2g})		
1258, 1269	1250, 1260	1240	anion, C−F stretch, ET ν_5 (A_g)	anion, C−F stretch + ET related ν_5 (A_g)	anion, C−F stretch
ω (cm^{-1}) $\parallel b$			assignment		
SC	M/I	M	SC	M/I	M
1257		1240	anion, C−F stretching		anion, C−F stretching
	1250[c]			anion, C−F stretch + ET related ν_5 (A_g)	

[a] References 9 and 10. [b] Note that these features are maxima in $\sigma_1(\omega)$ not unperturbed frequencies. [c] Peak at 1250 cm^{-1} in parallel polarization is possibly leakage from perpendicular polarization. Also, the large dip observed from ≈1200 to 1800 cm^{-1} in the $\parallel b$ direction of all three materials is assigned as a coupling of $\nu_3 + \nu_5$ modes of the ET molecule and can distort any anion feature that appears near it.

suggesting that the low-frequency strength of the other two samples has been redistributed in the R = $CHFCF_2$ material. This agrees with the reflectance spectra; the low-energy overdamped behavior of the metal and superconductor is replaced by a flat response in the metal/insulator material, with the additional broad excitation above 9000 cm^{-1}. This redistribution of oscillator strength is suggestive of electron localization on donor sites along the ET chain ($\perp b$ direction) in the metal/insulator material. Therefore, the bands at 4800 and 9500 cm^{-1} can be characterized as charge-transfer-type excitations in the dimerized ET chains. Because the anions in the R = CH_2CF_2 superconductor and R = CHF metal are ordered, whereas the anion in the R = $CHFCF_2$ metal/insulator is not, it is likely that disorder in the anion pocket is responsible for this localization of charge on the ET dimers in β''-$(ET)_2SF_5CHFCH_2SO_3$. That these excitations are explained within a localized model does not necessarily mean that they are correlation-driven. If many-body effects were the cause of this localization, a much higher effective mass would be expected for the metal/insulator material compared to the superconductor and metal. That the $\parallel b$ effective masses and overall structures for all three salts are so similar supports the "disorder" argument.

Thus, we propose that the 4800 and 9500 cm^{-1} excitations observed in the $\perp b$ reflectance and optical conductivity spectra of β''-$(ET)_2SF_5CHFCH_2SO_3$ are the result of electron localization on dimers of ET donor molecules driven by disorder in the anion pocket.[23] A similar doublet structure in a low-lying electronic band was observed in $(DIMET)_2SbF_6$ by Delhaes et al. and was assigned within a large U Hubbard approximation as intra- and interdimer charge-transfer excitations.[24] By analogy, the electronic feature at 9500 cm^{-1} in the metal/insulator material might be attributed to an excitation from lower to upper Hubbard bands. This excitation would be associated with the on-site Coulomb repulsion term U, which is essentially the energy required to doubly occupy a site. Theory predicts that there should be a simultaneous spectral enhancement corresponding to transitions from the lower Hubbard band to the central resonance at the Fermi level and from the Fermi level to the upper Hubbard band, both corresponding to an energy of $U/2$.[25] Thus, the electronic feature at 4800 cm^{-1} would be a good candidate for such an excitation; however, a trace of this feature is also observed in the $\perp b$ response of the other two materials, so that this assignment is less satisfying overall. Therefore, more work is needed before the 4800 cm^{-1} feature can be unambiguously assigned. Investigations of electronic charge transfer in composite β''-$(ET)_2SF_5RSO_3$ materials (with R = CH_2CF_2 and R = $CHFCF_2$ anions) are underway.

B. Vibrational Features. The behavior of a number of key vibrational modes in β''-$(ET)_2SF_5CH_2CF_2SO_3$, β''-$(ET)_2SF_5CHFCF_2SO_3$, and β''-$(ET)_2SF_5CHFSO_3$ is summarized in Table 1 for easy comparison.[9,10,26] While some features in this frequency range are anion modes coupled with ET vibrations, it is interesting that the majority of vibrational features are purely anion-related; it is uncommon to observe so many modes related to the counterion in low-dimensional organic solids. The prevalence of the anion-related features is likely due to the molecular (rather than polymeric) nature of the $SF_5RSO_3^-$ counterion.

Overall, the $\perp b$ vibrational response of the metal is most similar to that of the superconductor. The modes in the R = CHF metal are, however, stronger than those in the R = CH_2CF_2 superconductor and are slightly redshifted. The stronger vibrations along with the larger low-frequency $\perp b$ reflectance level of the metal underscore the fact that this material does not condense into the superconducting ground state. The R = $CHFCF_2$ metal/insulator material displays much stronger anion modes than the other two salts, and these modes are slightly broadened. The peak broadening is a direct consequence of the disordered anion pockets, which generate many different local environments for the anions and hence lead to a broadening of the anion

(23) The temperature-dependent reflectance of the metal/insulator material was reported by Olejniczak et al. (ref 10), and the low-lying electronic excitations found in the $\perp b$ polarization are characteristic features both above and below T_c = 180 K. Above 180 K, the material is considered a metal because of the characteristic behavior of the temperature-dependent resistivity; the actual conductivity is still very low. Below the 180 K transition, ρ is activated but the magnitude of the conductivity is similar to that above the transition. For comparison purposes, the 300 K ("metallic" regime) spectrum is presented here, but that does not mean that an assignment of localization is inappropriate.

(24) Delhaes, P.; Garrigou-Lagrange, C. *Phase Transitions* **1988**, *13*, 87.

(25) Rozenberg, M. J.; Kotliar, G.; Kajueter, H. *Phys. Rev. B* **1996**, *54*, 8452.

(26) The vibrational features of the β''-$(ET)_2SF_5RSO_3$ family are not well-resolved in the $\parallel b$ polarization, as the weakly metallic character partly screens most modes. The vibrational modes in the $\perp b$ polarization are highlighted here.

vibrational frequencies. The spectra of the metal/insulator also display concomitant electron−phonon-coupling-allowed features overlapping with the aforementioned anion vibrations. Strong electron−phonon coupling is consistent with charge-transfer excitations along the ET stack, providing further indication that the electronic features observed in the near-infrared regime of β″-(ET)$_2$SF$_5$CHFCF$_2$SO$_3$ result from (disorder-driven) charge localization in the ET stack direction.

While it is disorder in the anion pockets of β″-(ET)$_2$SF$_5$CHFCF$_2$SO$_3$ and β″-(ET)$_2$SF$_5$CHFSO$_3$ that prevents condensation into the superconducting ground state, there are much more disordered systems in which it is preserved. For example, samples of (BETS)$_2$MX$_4$ containing many different anions (such as MX$_4$ = GaBr$_4$, GaCl$_4$, FeCl$_4$, FeBr$_4$, etc.) show a superconducting transition. In contrast, the disordered ClO$_4$ ion in the TMTSF salt destroys the superconductivity.[1,27,28] In the β″-(ET)$_2$SF$_5$RSO$_3$ family of materials, it is *where* the disorder lies in the structure that plays a more important role in determining the ground-state properties, rather than the overall amount of disorder.

V. Conclusion

We report the polarized infrared reflectance, optical conductivity, and calculated band structures of β″-(ET)$_2$SF$_5$CHFSO$_3$ and compare them with those of β″-(ET)$_2$SF$_5$CHFCF$_2$SO$_3$ and β″-(ET)$_2$SF$_5$CH$_2$CF$_2$SO$_3$. The low-energy ⊥*b* excitations at 4800 and 9500 cm^{-1} found in the R = CHFCF$_2$ metal/insulator material are absent in the R = CHF and R = CH$_2$CF$_2$ compounds. These three salts are very similar in their calculated electronic band structures and ||*b* effective masses, thereby suggesting that the electronic excitations found in the metal/insulator material are caused by a disorder-driven charge localization on the ET stack. A detailed comparison of the vibrational features also supports this supposition. It is interesting to note that this disorder-driven localization causes low-energy excitations along the poorly conducting direction but not along the highly conducting direction. Thus, the most important and distinguishing spectral effects are in the transverse (least conducting) direction, in line with recent theoretical work done by Mazumdar, Clay, and Campbell.[29]

Acknowledgment. Work at SUNY-Binghamton was supported by Grant No. DMR-9623221 from the Division of Materials Research at the National Science Foundation. I.O. thanks the National Science Foundation and North Atlantic Treaty Organization for fellowship support (DGE 9804462). Work at Argonne National Laboratory and North Carolina State University was supported by Grant No. W-31-109-ENG-38 and Grant No. DE-FGO5-86ER45259, respectively, from the Division of Materials Science, Office of Basic Energy Sciences at the U.S. Department of Energy, and that at Portland State University was supported by the National Science Foundation (CHE-9904316) and the Petroleum Research Fund ACS-PRF No. 34624-AC7. This work has benefited from useful conversations with D. K. Campbell, R. T. Clay, and S. Mazumdar.

CM000349L

(27) Sato, A.; Ojima, E.; Akutsu, H.; Nakazawa, Y.; Kobayashi, H.; Tanaka, H.; Kobayashi, A.; Cassoux, P. *Phys. Rev. B* **2000**, *61*, 111.

(28) Montgomery, L. K.; Burgin, T.; Huffman, J. C.; Carlson, K. D.; Dudek, J. D.; Yaconi, G. A.; Megna, L. A.; Mobley, P. R.; Kwok, W. K.; Williams, J. M.; Schirber, J. E.; Overmyer, D. L.; Ren, J.; Rovira, C.; Whangbo, M.-H. *Synth. Met.* **1993**, *55*−*57*, 2090.

(29) Mazumdar, S.; Clay, R. T.; Campbell, D. K. cond-mat/0003200, 2000.